

## Diffraction Management

H. S. Eisenberg and Y. Silberberg

*Department of Physics of Complex Systems, The Weizmann Institute of Science, 76100 Rehovot, Israel*

R. Morandotti and J. S. Aitchison

*Department of Electronics and Electrical Engineering, University of Glasgow, Glasgow G12 8QQ, Scotland*

(Received 9 March 2000)

By using the diffraction properties of waveguide arrays, we propose a scheme to produce structures with designed diffraction. We fabricated arrays with reduced, canceled, and even reversed diffraction. Results of experiments with such waveguides are presented and compared with the predictions made by coupled-mode theory.

PACS numbers: 42.25.Fx, 42.79.Gn, 42.82.Et

Optical diffraction and dispersion originate from physically different sources, but share many common properties. Both effects lead to the broadening of an initial intensity profile, either in space by diffraction or in time by dispersion. Both phenomena arise due to different rates of phase accumulation for different (spatial, or temporal) frequencies. Dispersion is material dependent: it is zero in vacuum and in certain materials at specific wavelengths. On the other hand, diffraction is a geometrical effect and depends only weakly on the medium the light propagates in, via its refractive index.

Dispersion can be controlled by changing materials and/or geometry of a waveguide. For example, optical glass fibers can be engineered to cancel dispersion and even change its sign [1]. By alternate use of fibers of positive and negative dispersion, transmission lines of managed dispersion have been demonstrated [2–4]. Because dispersion is a linear phenomenon, the accumulative dispersion of cascaded different fibers is equivalent to propagation in a fiber with an averaged dispersion.

Unlike dispersion, diffraction exists even in vacuum due to its geometrical origin. In the far field, a Gaussian beam with a waist  $w_0$  broadens with an angle of  $\theta_{\text{ff}} = \lambda_0/\pi w_0 n$ , where  $\lambda_0$  is the wavelength in vacuum and  $n$  is the linear refractive index [5]. To date, there is no way to control the expansion rate of a given beam other than by changing the refractive index of the material. Canceling diffraction, or changing its sign are impossible via this method. It is the purpose of this paper to suggest and demonstrate a way of designing an arbitrary diffraction relation in a planar waveguide, which can even produce zero and reversed values.

Consider the propagation of scalar plane waves of the form  $E(\vec{r}) = E_0 \exp(i\vec{k} \cdot \vec{r})$  in a two-dimensional free space, where  $\vec{k}$  is the wave vector whose  $x$  and  $z$  components are  $k_x$  and  $k_z$ , respectively [6]. The absolute value of  $\vec{k}$  is  $k = \frac{2\pi n}{\lambda_0}$  and it points along the normal to the plane wave phase fronts. In analogy with the dispersion relation, we can define the diffraction relation of the time independent optical wave equation [7] (see Fig. 1):

$$k_z(k_x) = \sqrt{k^2 - k_x^2}, \quad (1)$$

which can also be derived from basic geometrical considerations. For  $k_x \ll k$ , it is common to make the paraxial approximation, and the diffraction relation (equivalent to the Helmholtz equation) becomes

$$k_z = k - \frac{k_x^2}{2k}. \quad (2)$$

When an optical field propagates over a distance  $z$ , each transverse component  $k_x$  gains a phase  $\phi(k_x, z) = k_z(k_x)z$ . A group of transverse components centered at  $k_x$  is shifted by an amount  $\Delta x = \frac{\partial \phi}{\partial k_x} = \frac{\partial k_z}{\partial k_x} z$ , i.e., the propagation direction is simply  $\alpha = \tan^{-1}(\frac{\partial k_z}{\partial k_x})$ . The field broadens because of the divergence between different displacements  $D = \frac{1}{z} \frac{\partial^2 \phi}{\partial k_x^2} = \frac{\partial^2 k_z}{\partial k_x^2}$ , which we term diffraction in analogy to the definition of dispersion. This difference in transverse shifts between spatial frequency components of a limited

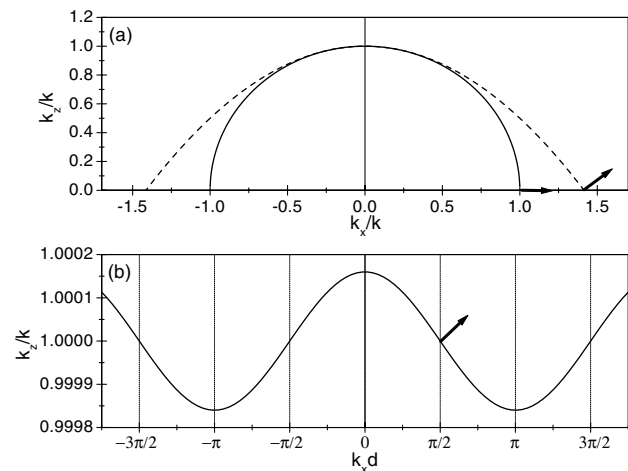


FIG. 1. Diffraction curves: phase vs spatial frequency for various models. The arrows mark the largest possible angle of energy propagation for each model. (a) Diffraction in a homogeneous medium, nonparaxial (solid line) and paraxial (dashed line). (b) discrete diffraction. Clearly, paraxiality fails beyond  $\sim 0.5k$ . Only discrete diffraction exhibits inversion of curvature around  $\pm\pi/2$ .

size optical field is the reason for the broadening of light beams, the diffraction patterns of apertures, and similar phenomena. The Poynting vector of each  $k_x$  component in real space is directed perpendicular to the diffraction curve, which is circular in the nonparaxial case [8].

The diffraction in free space is  $D_{np} = \frac{-k^2}{(k^2 - k_x^2)^{3/2}}$ , which is simplified in the paraxial limit to  $D_p = -\frac{1}{k}$ . Note that  $D_p$  does not depend on  $k_x$  and is always negative. This expression for paraxial diffraction resembles the approximation of temporal dispersion using a second order expansion. One immediate consequence is the possibility of generating solitons under nonlinear propagation [9]. The sign of diffraction is always negative, hence only *bright* spatial solitons form in materials with a focusing Kerr nonlinearity. On the other hand, *dark and bright* temporal solitons can exist in normal and anomalous dispersive materials, respectively.

Consider now the case of optical field propagation in a linearly coupled, infinite array of one dimensional waveguides. The diffraction relation of such an array can be derived from the optical equivalent of the continuous model of tight binding of electrons in a one dimensional atomic lattice [10]. The optical coupled mode set of equations for the electrical field in the  $n$ th waveguide and the consequent diffraction relation are [11,12]

$$\frac{dE_n}{dz} = ik_{wg}E_n + iC(E_{n-1} + E_{n+1}), \quad (3)$$

$$k_z = k_{wg} + 2C \cos(k_x d).$$

In Eqs. (3),  $k_{wg}$  is the propagation constant of the waveguide,  $d$  is the distance between the centers of two adjacent waveguides, and  $C$  is the coupling constant between them, which is proportional to an overlap integral of the two modes of such waveguides. Accordingly, the *discrete diffraction* is  $D_d = -2Cd^2 \cos(k_x d)$ . Paraxiality is implicitly assumed in the derivation of Eqs. (3), and it is valid as long as  $C \ll k$ . Nevertheless, paraxiality is not necessary for the ideas presented here. A Brillouin zone is formed in the range  $|k_x d| < \pi$  and any higher frequency has an equivalent inside it (see Fig. 1b). Note that because of the periodicity and the continuity of the diffraction relation, there exists a maximal angle of propagation for the light energy,  $\alpha_{\max} \approx 2Cd$ . The eigenmodes of this diffraction relation [Eqs. (3)] are known as Floquet-Bloch waves, first introduced in the dynamical theory of x-ray diffraction [13]. Floquet-Bloch waves were used in optics in the past for describing the propagation of light in corrugated planar waveguides both in time [14] and space [8,15], and also in a two dimensional optical lattice [16]. Notice that the Floquet-Bloch treatment is not derived by assuming the tight binding model, but rather by a weak periodic potential [10]. Nevertheless, as in solid state physics, both approaches lead to the same qualitative results [14,17]. Optical waveguide arrays have more similarities to electrons in an atomic lattice, such as the appearance of Bloch oscillations which was demonstrated recently [18,19].

The most important feature of Eqs. (3) in the current context is the inversion of the sign of the diffraction  $D_d$  in the outer parts of the Brillouin zone. Diffraction becomes positive in the range  $\frac{\pi}{2} < |k_x d| \leq \pi$ , enabling light beams to experience *anomalous* diffraction, i.e., of opposite sign to that experienced in nature. Moreover, diffraction completely disappears around the two points  $k_x = \pm \frac{\pi}{2d}$ . Recently, a similar effect was shown to happen in photonic crystals [20].

We first demonstrate the basic properties of discrete diffraction. Arrays of 61 single-mode strip waveguides were fabricated on top of a planar waveguide. The slab waveguide consists of a  $1.5 \mu\text{m}$  layer of  $\text{Al}_{0.18}\text{Ga}_{0.82}\text{As}$  core between two  $\text{Al}_{0.24}\text{Ga}_{0.76}\text{As}$  cladding layers of  $1.5$  and  $4 \mu\text{m}$ . The waveguides were patterned by etching  $0.95 \mu\text{m}$  of the upper  $1.5 \mu\text{m}$  cladding, thus lowering the effective refractive index below the etched area. Each strip waveguide is  $4 \mu\text{m}$  wide and the separations between their centers were either  $8$  or  $9 \mu\text{m}$ . Arrays were tilted from the normal to the input facet, to achieve easy coupling condition into specific  $k_x$  range of modes. The angles corresponded to various values  $\theta = k_x d$  in the range of  $0$  to  $\pi$  [ $\pi$  equivalent to a tilt angle of  $\alpha = \sin^{-1}(\frac{\theta}{kd}) \approx 1.5^\circ$  in our configuration]. Light was injected using a  $\times 40$  objective and cylindrical optics in order to shape the input beam. Images of the output facet of the sample were taken with an IR camera. All experiments were done using a synchronously pumped optical parametric oscillator (OPO) tuned to a wavelength of  $1.53 \mu\text{m}$ .

Cross sections of the output fields from samples with  $d = 9 \mu\text{m}$  ( $3.0$  coupling lengths in the  $6 \text{ mm}$  long sample) are presented in Fig. 2. The input Gaussian beam [21] with  $w_0 = 21 \mu\text{m}$  excited mostly three waveguides. The beam expanded to  $42 \mu\text{m}$  when propagating in the untilted array. In comparison, it expanded to  $54 \mu\text{m}$  in a continuous slab waveguide. For  $\theta = \frac{\pi}{2}$ , where diffraction should vanish, the output field broadened to only

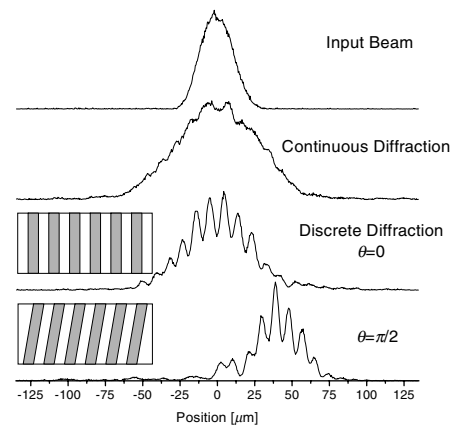


FIG. 2. Input and output intensity profiles. Input beam was  $21 \mu\text{m}$  wide. Under continuous and normal discrete diffraction, the beam expands by about a factor of 2. At zero diffraction condition, the broadening is mainly due to remanent higher orders. Inset: A sketch of the waveguides.

29  $\mu\text{m}$ . It also exhibited an asymmetric profile, attributed to the remanent third order diffraction. This field shape resembles the temporal shape of an optical pulse after traveling in a “zero dispersion” fiber, experiencing mostly third order dispersion [22].

We propose to use these properties in order to design structures with a customized diffraction relation. Borrowing the idea of dispersion management from optical fiber technology [2], we suggest to use the cascading of different short segments of waveguide arrays in order to achieve a desired average diffraction. The diffraction relation of each segment is determined by three physical parameters, namely the period, the coupling strength, and the tilt angle. The array period determines the frequency of the cosine in the diffraction curve [Eqs. (3)], the tilt angle determines the phase, and the coupling between waveguides and the array length affects its amplitude. Therefore, in order to design a waveguide with a specific diffraction curve, one should span the desired curve with the appropriate Fourier series of cosine and sine functions and fabricate a cascade of the corresponding angled arrays. The segment’s length can be much shorter than the overall length, as long as it is not comparable to the waveguide spacing  $d$ . For diffraction management, in contrast with just diffraction compensation, the segments need to be shorter than the coupling length  $\pi/2C$ .

One simple realization of these ideas is a sequence of arrays with alternating tilt angles. In such a structure, the dominant diffraction term  $D_d$  can be controlled without significant contribution from higher orders. In particular, for  $\theta = \frac{\pi}{2}$  the average diffraction curve is

$$\langle D_z \rangle = -Cd^2 \left[ \cos\left(k_x d - \frac{\pi}{2}\right) + \cos\left(k_x d + \frac{\pi}{2}\right) \right] = 0. \quad (4)$$

This implies a complete cancellation of all orders of diffraction.

Arrays of zigzag waveguides, 5 and 6 mm long, were fabricated. The structure was segmented into 200  $\mu\text{m}$  long sections, tilted alternately by  $\alpha$  and  $-\alpha$ . Arrays with the same range of angles as before were tested, but this time  $d = 8 \mu\text{m}$  (4.2 coupling lengths). Results for 5 and 21  $\mu\text{m}$  input beams are presented in Figs. 3 and 4, respectively. The narrow input excites a broader band of spatial frequencies. All curves are normalized to have the same maximum value. The absence of diffraction at  $\theta = \frac{\pi}{2}$  is obvious. The output field profile of a zero diffraction waveguide resembles the input field, and it is significantly narrower than the field coming out of a straight array ( $\theta = 0$ ). Note that the broad beam produces a smoother, low background output. Although it behaves much like a continuous beam, it expands according to discrete diffraction. The results are compared to two numerical solutions of the problem: a coupled-mode theory (CMT) solution [23] of a finite set of ordinary differential equations (ODE’s) with the Runge-Kutta method and a 2D beam propaga-

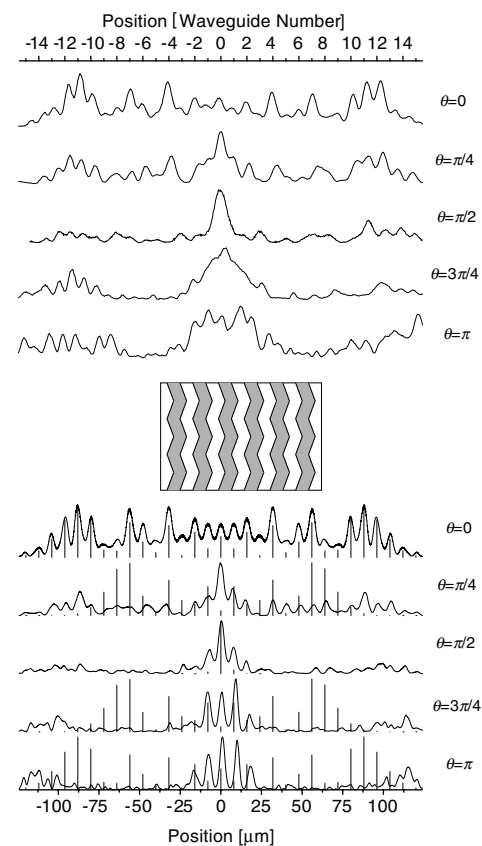


FIG. 3. Output intensity profiles after propagation of a 5  $\mu\text{m}$  wide input through zigzag arrays. Upper graph: Experimental results for various tilt angles. Lower graph: Calculated output by beam propagation method (continuous lines) and coupled mode theory (vertical bars). Inset: A sketch of the waveguides.

tion method (BPM) for solving the evolution of the optical field. The experimental results match the BPM solution quite well, while deviating from the CMT solution for  $\theta$  larger than  $\frac{\pi}{2}$  and for the broader beam also for  $\theta = 0$ . The Floquet-Bloch analysis predicts a second diffraction branch (band, in the solid state analogy) that spans the spatial modes which are complementary to the waveguide modes. The second branch modes have maxima in between the waveguides and lower propagation constants  $k_z$ . They are not included in the CMT analysis. The sign of diffraction in the second branch  $D_d^{II}$  is generally opposite to that of the first branch  $D_d$ . For angles approaching  $\pi$  the two branches are closer and more light is coupled to the second branch, hence CMT is expected to fail. The sharp turn point of the zigzag waveguides also contributes to the transfer of energy between the branches. Because BPM simulation solves the propagating field directly, it fits much better than CMT to the experimental results.

Controlled diffraction can be useful in many situations. For example, the spatial equivalent of the temporal stretched-pulse amplifier can be built using a semiconductor optical amplifier in order to increase saturation powers. A beam should be first broadened by a waveguide with normal diffraction, and after amplification it could be

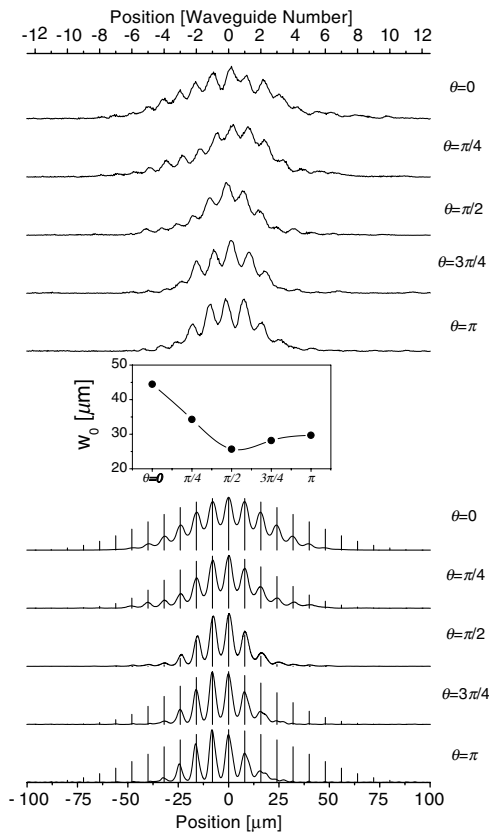


FIG. 4. Same as Fig. 3 for a  $21 \mu\text{m}$  wide input. Inset: widths for the experimental output profiles.

compressed using diffraction of the opposite sign. Also, in planar waveguide lasers, where nonlinear filamentation is limiting the output power level, negative diffraction could eliminate modulational instability and the waveguide will be self-defocusing.

Diffraction relation can be engineered to have an arbitrary shape by a series of arrays with different spacings. For example, a triangular shaped diffraction leads to propagation without diffraction, in only two specific directions. Such a periodic triangular function is spanned by the series  $\sum_n \frac{\cos[(2n-1)k_x d]}{(2n-1)^2}$ , which can be approximated well by just the first two terms. Note that such a structure requires alternating waveguides with different periods, however, we have previously verified experimentally that coupling efficiency is almost unaffected by the array structure [24].

The ability to engineer diffraction opens several possibilities for spatial soliton physics. Dark solitons in self-focusing media can be demonstrated in negative diffraction geometries [25]. Diffraction managed spatial solitons [3,4] could be formed at powers much smaller than those which are required in slab waveguides. This kind of spatial soliton can be the building block for low power all-optical soliton switches.

In conclusion, by borrowing ideas from dispersion management, we propose a technique to exploit the negative curvature of the diffraction curve of light in waveguide

arrays in order to control diffraction. We fabricated and demonstrated waveguides with diminished, canceled, and reversed diffraction. We believe that the ability to control diffraction could prove useful to various linear and non-linear guided wave devices.

The authors would like to thank D.N. Christodoulides for helpful discussions. We also gratefully acknowledge support from the Israeli Ministry of Science and the U.K. Engineering and Physical Science Research Council.

- [1] L. G. Cohen, C. Lin, and W. G. French, *Electron. Lett.* **15**, 334 (1979).
- [2] C. Lin, H. Kogelnik, and L. G. Cohen, *Opt. Lett.* **5**, 476 (1980).
- [3] F. M. Knox, W. Forsysiak, and N. J. Doran, *J. Lightwave Technol.* **13**, 1955 (1995).
- [4] I. R. Gabitov and S. K. Turitsyn, *Opt. Lett.* **21**, 327 (1996).
- [5] H. Kogelnik and T. Li, *Appl. Opt.* **5**, 1550 (1966).
- [6] We limit the discussion here to two-dimensional propagation for simplicity, although this approach is straightforwardly extendable to three dimensions (see Ref. [16]).
- [7] J. D. Jackson, *Classical Electrodynamics* (John Wiley & Sons, New York, 1975), 2nd ed.
- [8] P. St. J. Russell, *Appl. Phys. B* **39**, 231 (1986).
- [9] A. Hasegawa and F. Tappert, *Appl. Phys. Lett.* **23**, 142 (1973); **23**, 171 (1973).
- [10] N. W. Ashcroft and N. D. Mermin, *Solid State Physics* (Holt, Rinehart & Winston, New York, 1976).
- [11] S. Somekh, E. Garmire, A. Yariv, H. L. Garvin, and R. G. Hunsperger, *Appl. Phys. Lett.* **22**, 46 (1973).
- [12] D. N. Christodoulides and R. I. Joseph, *Opt. Lett.* **13**, 794 (1988). For a recent review, see *Optical Solitons: Theoretical Challenges and Industrial Perspectives*, edited by V. E. Zakharov and S. Wabnitz (Springer-Verlag, Berlin, 1999).
- [13] J. M. Cowley, *Diffraction Physics* (Elsevier Science B.V., Amsterdam, 1995), 3rd revised ed.
- [14] A. Yariv and A. Gover, *Appl. Phys. Lett.* **26**, 537 (1975).
- [15] P. St. J. Russell, *Phys. Rev. A* **33**, 3232 (1986).
- [16] J. Feng and N. B. Ming, *Phys. Rev. A* **40**, 7047 (1989).
- [17] P. St. J. Russell, *Opt. Commun.* **48**, 71 (1983).
- [18] R. Morandotti, U. Peschel, J. S. Aitchison, H. S. Eisenberg, and Y. Silberberg, *Phys. Rev. Lett.* **83**, 4756 (1999).
- [19] T. Pertsch, P. Dannberg, W. Elflein, A. Bräuer, and F. Lederer, *Phys. Rev. Lett.* **83**, 4752 (1999).
- [20] H. Kosaka, T. Kawashima, A. Tomita, M. Notomi, T. Tamamura, T. Sato, and S. Kawakami, *Appl. Phys. Lett.* **74**, 1212 (1999).
- [21] We present results in terms of their Gaussian width  $w_0$ , which is related to the full width half maximum by  $\sim 1.17w_0$ .
- [22] M. Miyagi and S. Nishida, *Appl. Opt.* **18**, 678 (1979).
- [23] A. Yariv, *IEEE J. Quantum Electron.* **9**, 919 (1973).
- [24] R. Morandotti, U. Peschel, J. S. Aitchison, H. S. Eisenberg, and Y. Silberberg, *Phys. Rev. Lett.* **83**, 2726 (1999).
- [25] Y. S. Kivshar, W. Królikowski, and O. A. Chubykalo, *Phys. Rev. E* **50**, 5020 (1994).